



1 **Oxygenated VOCs as significant but varied contributors**
2 **to VOC emissions from vehicles**

3 Sihang Wang^{1,2}, Bin Yuan^{1,2,*}, Caihong Wu^{1,2}, Chaomin Wang^{1,2}, Tiange Li^{1,2}, Xianjun
4 He^{1,2}, Yibo Huangfu^{1,2}, Jipeng Qi^{1,2}, Xiaobing Li^{1,2}, Junyu Zheng^{1,2}, Qing'e Sha^{1,2},
5 Manni Zhu^{1,2}, Shengrong Lou³, Hongli Wang³, Thomas Karl⁴, Martin Graus⁴, Zibing
6 Yuan^{5*}, Min Shao^{1,2}

7 ¹ Institute for Environmental and Climate Research, Jinan University, Guangzhou
8 511443, China

9 ² Guangdong-Hongkong-Macau Joint Laboratory of Collaborative Innovation for
10 Environmental Quality, Guangzhou 511443, China

11 ³ State Environmental Protection Key Laboratory of Formation and Prevention of
12 Urban Air Pollution Complex, Shanghai Academy of Environmental Sciences,
13 Shanghai 200233, China

14 ⁴ Department of Atmospheric and Cryospheric Sciences, University of Innsbruck,
15 Innsbruck, Austria

16 ⁵ College of Environment and Energy, South China University of Technology,
17 University Town, Guangzhou 510006, China

18
19
20 *Correspondence to: Bin Yuan (byuan@jnu.edu.cn) and Zibing Yuan
21 (zibing@scut.edu.cn)

22



23 **Abstract:**

24 Vehicular emission is an important source for volatile organic compounds (VOCs) in
25 urban and downwind regions. In this study, we conducted a chassis dynamometer study
26 to investigate VOC emissions from vehicles using gasoline, diesel, and liquefied
27 petroleum gas (LPG) as fuel. Time-resolved VOC emissions from vehicles are
28 chemically characterized by a proton-transfer-reaction time-of-flight mass
29 spectrometry (PTR-ToF-MS) with high frequency. Our results show that emission
30 factors of VOCs generally decrease with the improvement of emission standard for
31 gasoline vehicles, whereas variations of emission factors for diesel vehicles with
32 emission standards are more diverse. Mass spectra analysis of PTR-ToF-MS suggest
33 that cold start significantly influence VOCs emission of gasoline vehicles, while the
34 influences are less important for diesel vehicles. Large differences of VOC emissions
35 between gasoline and diesel vehicles are observed with emission factors of most VOC
36 species from diesel vehicles were higher than gasoline vehicles, especially for most
37 oxygenated volatile organic compounds (OVOCs) and heavier aromatics. These results
38 indicate quantification of heavier species by PTR-ToF-MS may be important in
39 characterization of vehicular exhausts. Our results suggest that VOC pairs (e.g. C₁₄
40 aromatics/toluene ratio) could potentially provide good indicators for distinguishing
41 emissions from gasoline and diesel vehicles. The fractions of OVOCs in total VOC
42 emissions are determined by combining measurements of hydrocarbons from canisters
43 and online observations of PTR-ToF-MS. We show that OVOCs contribute $7.7\% \pm 6.2\%$
44 of gasoline vehicles of the total VOC emissions, while the fractions are significantly
45 higher for diesel vehicles (40-77%), highlighting the importance to detect these OVOC
46 species in diesel emissions. Our study demonstrated that the large number of OVOC
47 species measured by PTR-ToF-MS are important in characterization of VOC emissions
48 from vehicles.

49



50 1. Introduction

51 Volatile organic compounds (VOCs) are important trace components in the
52 troposphere, as important precursors of ground-level ozone (Shao et al., 2009) and
53 secondary organic aerosol (SOA) (Seinfeld and Pandis, 2006;Kansal, 2009;Ziemann
54 and Atkinson, 2012). As the result, it is particularly important to identify emission
55 sources of VOCs in the atmosphere. Vehicular emission is an important source of VOCs
56 in cities around the world (Liu et al., 2008;Parrish et al., 2009), contributing
57 approximately 25% to total VOC emissions in China (Ou et al., 2015;Wu et al.,
58 2016;Sun et al., 2018). In order to control atmospheric pollution in urban and
59 surrounding regions, it is necessary to understand source profiles and emission
60 characteristics of VOCs from vehicles.

61 Emissions of VOCs from vehicles have been investigated extensively from
62 tunnel studies (Cui et al., 2018;Zhang et al., 2018;Song et al., 2020), on-road mobile
63 measurements (Li et al., 2017), and chassis dynamometer tests (Guo et al., 2011;Wang
64 et al., 2013;Yang et al., 2018). Previous studies demonstrated that fuel types of vehicles
65 strongly impact VOC emissions. Aromatics along with other hydrocarbons are known
66 as compounds with high emissions in exhausts of gasoline vehicles (Wang et al.,
67 2013;Ly et al., 2020). Some carbonyl compounds contribute significantly to emissions
68 of diesel vehicles, at fractions much higher than gasoline vehicles (Tsai et al., 2012;Qiao
69 et al., 2012;Yao et al., 2015;Mo et al., 2016). Moreover, there are still a large number
70 of unidentifiable compounds in diesel vehicles (May et al., 2014). Furthermore, VOC
71 emissions significantly decreased for stricter emission standards (Cao et al., 2016). In
72 order to reduce emissions of most primary pollutants, more stringent emission standards
73 and after-treatment devices have been implemented. The emission standard of China
74 VI has already been implemented in July of 2019 in a few key cities in China and in
75 July of 2021 nationwide. The emission limits for various air pollutants emitted by
76 vehicles are significantly lower under the China VI emission standard (Wu et al., 2017).
77 With the continuous development of engine and exhaust after-treatment technologies,
78 emission characteristics of VOCs from vehicles may change and need to be frequently



79 updated.

80 Oxygenated volatile organic compounds (OVOCs) were found to be an important
81 group in vehicle exhausts, accounting for more than 50% of the total VOC emissions
82 for diesel vehicles (Schauer et al., 1999; Yao et al., 2015; Mo et al., 2016). Traditionally,
83 VOCs are collected in the canister or Tedlar bags, and then analyzed by gas
84 chromatography-mass spectrometer/flame ionization detector (GC-MS/FID), mainly
85 reporting emissions of hydrocarbons (Wang et al., 2017; Qi et al., 2019). Previous work
86 usually collected 2,4-dinitrophenylhydrazine (DNPH) cartridges and analyzed using
87 high-performance liquid chromatography (HPLC) for carbonyls (aldehydes and
88 ketones), which are both time-consuming and prone to contaminations (Mo et al.,
89 2016; Han et al., 2019).

90 The large variability of VOC emissions under different engine activities or
91 driving conditions require characterization of vehicular emissions at higher time
92 resolution. Proton-transfer-reaction mass spectrometry (PTR-MS) has been used in a
93 number of studies for measurements of vehicle emissions. VOCs from vehicle exhausts
94 under various driving and operational modes were measured by PTR-MS onboard a
95 mobile laboratory (Zavala et al., 2006; Zavala et al., 2009). Drozd et al. (2016) used a
96 PTR-MS to emphasize the importance of cold start for vehicles, concluding that VOC
97 emissions during cold start were equal to a 200 miles distance of driving during hot
98 stabilized condition. Proton-transfer-reaction time-of-flight mass spectrometry (PTR-
99 ToF-MS) can provide more powerful detection of various VOCs, thanks to the
100 measurements of whole mass spectra and high mass resolution (Cappellin et al.,
101 2012; Yuan et al., 2017). More OVOC species could be quantified from the measured
102 mass spectra based on parameterization methods for sensitivity of instrument
103 (Sekimoto et al., 2017; Wu et al., 2020).

104 In this study, we applied a PTR-ToF-MS along with a suite of other instruments
105 to measure VOCs emitted from gasoline, diesel, and liquefied petroleum gas (LPG)
106 vehicles. We investigated emission factors from different fuel types and emission
107 standards for representative VOC species exhausted from these vehicles. We used the
108 dataset to analyze contributions of various VOC groups to total VOC emissions in



109 different types of vehicles.

110 **2. Materials and methods**

111 **2.1 Tested vehicles and the chassis dynamometer study methods**

112 In this study, we conducted chassis dynamometer measurements to investigate
113 VOC emissions from vehicles using gasoline, diesel, LPG as fuel. All gasoline vehicles
114 are light-duty-gasoline-vehicle (LDGV) with the emission standards from China I to
115 China VI, whereas diesel vehicles can be classified into light-duty-diesel-truck (LDDT),
116 middle-duty-diesel-truck (MDDT), heavy-duty-diesel-truck (HDDT), and bus
117 associated with emission standards of China III to China V. In addition, the test vehicles
118 using LPG are all taxis, which are under mandatory scrappage after 8 years of driving
119 in China; as a result only China IV and China V for LPG vehicles were tested. Among
120 the 38 vehicles we tested, a fraction of vehicles was measured several times, with a total
121 of 62 experiments measured. The detailed information for test vehicles is summarized
122 in Table S1 and Table S2.

123 The short transient driving cycle (GB 18285-2018, Figure S1a), as one of the
124 widely used test methods for vehicle emissions in China (Li et al., 2012; Wang et al.,
125 2013), was used for measurements of gasoline vehicles and LDDT, each running for
126 three to five times. The short transient driving cycle methods were initially adapted
127 based on emission regulations of the Economic Commission for Europe (ECE) cycle
128 (Yao et al., 2003), which is developed and used in European countries (Laurikko, 1995).
129 The short transient driving cycle consist of four conditions, namely idling, acceleration,
130 deceleration and uniform speed, as shown in Fig. S1. For the MDDT and HDDT, we
131 customized a step-by-step test method, in which the vehicle accelerates to 20 km·h⁻¹,
132 40 km·h⁻¹ and 60 km·h⁻¹ in sequence after the engine activates, keeping at 20 km·h⁻¹
133 and 40 km·h⁻¹ for 2 minutes, and 60 km·h⁻¹ for 1 minute, respectively (Fig. S1) (Li et
134 al., 2021; Liu et al., 2021; Liao et al., 2021). In addition, the cold start was tested for a
135 number of vehicles after a cold soak for more than 12 hours at ambient temperature
136 (20-25 °C) before engine started. The measurements of cold start are compared to
137 measurements of hot start after a ~10 minutes break for the vehicles after previous



138 measurement. More details about cold start and hot start in this campaign can be found
139 in Li et al. (2021).

140 A custom-built sampling and dilution system for vehicles combining online and
141 offline sampling techniques was used in this study. As shown in Fig. S2, a portable
142 emission measurement system (PEMS, SEMTECH-DS, Sensors. USA) was employed
143 to measure emissions of CO, CO₂, NO_x, and total hydrocarbon (THC) directly from the
144 tailpipe of vehicles. A custom-built dilution system (Li et al., 2021; Liao et al., 2021)
145 was used for dilution of vehicular emissions, achieving dilution ratios of 10-100 for
146 different vehicles. After dilution, CO₂ and CO were measured using a Li-840A
147 CO₂/H₂O Gas Analyzer (Licor, Inc. USA) and a Thermo 48i-TLE analyzer (Thermo
148 Fisher Scientific Inc. USA), respectively. Measurements of CO₂ before and after the
149 dilution system was used to determine the dilution ratio for each test (see details in Fig.
150 S3).

151 2.2 VOC measurements using PTR-ToF-MS

152 In this study, a Proton Transfer Reaction Quadrupole interface Time-of-Flight
153 Mass Spectrometer (PTR-QiToF-MS) (Ionicon Analytik, Innsbruck, Austria) with
154 H₃O⁺ chemistry was used to measure VOCs (Sulzer et al., 2014). The mass spectra of
155 PTR-ToF-MS was recorded every 1 s as to capture characteristics of VOC species from
156 vehicle exhausts in real-time. Background measurements of the instrument were
157 performed using sampled air through a custom-built platinum catalytical converter
158 heated to 365 °C for 30 s before vehicle starts in each test. The more detailed setting
159 parameters for the instrument can be found elsewhere (Wu et al., 2020; Wang et al.,
160 2020a; He et al., 2022). Data analysis of PTR-ToF-MS was performed using the Tofware
161 software package (version 3.0.3, Tofwerk AG, Switzerland) (Stark et al., 2015).

162 A 23-component gas standard (Linde Spectra) was used for daily calibration of
163 PTR-ToF-MS during the campaign. VOC sensitivities from automatical calibrations
164 indicated quite stable instrumental performance for most of the VOC species (Fig. S4).
165 Another gas standard with 35-component VOCs (Apel Riemer Environmental Inc.) was
166 used for calibrations during the later period of this campaign to include more VOC



167 species in the calibration. The Liquid Calibration Unit (LCU, Ionicon Analytik,
168 Innsbruck, Austria) was used to calibrate a total of 11 organic acids and nitrogen-
169 containing species (Table S3). The limits of detection for calibrated VOC species are
170 below 100 ppt for the 1-s measurement, except for ethanol (423 ppt) and formic acid
171 (166 ppt). Additionally, the humidity dependence for a few VOC species in PTR-ToF-
172 MS (Yuan et al., 2017;Koss et al., 2018) were corrected using humidity-dependence
173 curves determined in the laboratory, as previously shown in Wu et al. (2020). To
174 quantify the ion signals without calibration, we determine the sensitivities based on the
175 kinetics of proton-transfer reactions of H_3O^+ with VOCs (Cappellin et al.,
176 2012;Sekimoto et al., 2017). The relationship between VOCs sensitivity and kinetic
177 rate constants for the same instrument has been reported in Wu et al. (2020) and He et
178 al. (2022). The corrected sensitivities as a function of kinetic rate constants for proton-
179 transfer reactions of H_3O^+ with VOCs during this campaign is shown in Fig. S5. The
180 fitted line is used to determine sensitivities of uncalibrated species, and the uncertainty
181 of the concentrations for uncalibrated species are determined to be around 50%.

182 **2.3 Other VOC measurements**

183 Whole air samples were collected using canisters after the dilution system for
184 determination of hydrocarbons emitted from various vehicles. All the canisters were
185 sent to the laboratory for analysis by an offline GC-MS/FID system, with a total 95
186 hydrocarbons calibrated by Photochemical Assessment Monitoring Stations (PAMS)
187 and TO-15 standard mixtures (Table S4). Due to the difference of sampling (e.g., times
188 and dilution ratios), we compared emission factors from PTR-ToF-MS and the offline
189 canister-GC-MS/FID, obtaining consistent results, except for gasoline vehicles with
190 China I (Fig. S6c).

191 An instrument based on Hantzsch reaction-absorption method was used to
192 measure formaldehyde (Zhu et al., 2020). Good agreement for formaldehyde between
193 PTR-ToF-MS and the Hantzsch instrument was obtained (Fig. S6a). An iodide-adduct
194 time-of-flight chemical ionization mass spectrometer (I^- ToF-CIMS, Aerodyne
195 Research, Inc.) (Wang et al., 2020c;Ye et al., 2021) was used to measure organic acids,



196 hydrogen cyanide (HCN), and isocyanic acid (HNCO) from vehicles (Li et al., 2021).
197 As shown in Fig. S6b, formic acid measured by PTR-ToF-MS and I⁻ ToF-CIMS showed
198 reasonable agreement.

199 **2.4 Emission factors and emission ratios calculation**

200 In this study, we determine emission factors of VOC species in two different
201 approaches: the mileage-based emission factors ($\text{mg}\cdot\text{km}^{-1}$) as the mass of these VOCs
202 exhausted per kilometer driving of vehicles, and the fuel-based emission factors
203 ($\text{mg}\cdot\text{kg}_{\text{fuel}}^{-1}$) as the mass of VOCs per kilogram of fuel burned by the vehicles. In
204 addition, emission ratios of VOCs to combustion tracers (usually CO) are widely
205 applied in vehicle emissions in urban regions, as the result we determine emission
206 ratios to CO in $\text{ppb}\cdot\text{ppm}^{-1}$ as well. More details about the determination of emission
207 factors and emission ratios can be found in Sect. 1 in the Supplement.

208 The average emission factors for various types of vehicles are determined from
209 arithmetic means for different emission standards of vehicles. As for diesel vehicles,
210 the average emission factors are obtained from the arithmetic means of LDDT, MDDT,
211 HDDT, and bus. Besides, we also calculate emission factors and emission ratios from
212 weighted means based on the fractions of gasoline and diesel vehicles with different
213 emission standards in China (MEEPRC, 2019; Li et al., 2021) (See Sect. 1 in the
214 Supplement for details). In order to evaluate the uncertainties of obtained emission
215 factors, the average limit of detection for VOC species are used to estimate the limit
216 of detection for the determined emission factors (more details can be found in Sect. 2
217 in the Supplement).

218 **3. Results and discussions**

219 **3.1 Characteristics of the VOC emissions in the vehicles**

220 Time series of several aromatics and OVOC species measured by PTR-ToF-MS
221 for a selected gasoline vehicle associated with emission standard of China I and a LDDT
222 associated with China IV emission standard are shown in Fig. 1. Both tests started with
223 cold engines for the two vehicles. Benzene and toluene are typical aromatic species
224 exhausted by vehicles. As shown in Fig. 1a, high concentrations of benzene and toluene



225 exhausted by the gasoline vehicle were observed as the engine started. The
226 concentrations of the two species continued to increase until ~2 min after the engine
227 started, and then dropped rapidly before a minor increase during the acceleration
228 condition. These observations are similar to the previous results from PTR-MS
229 measurements in Drozd et al. (2016). Acetaldehyde and acetone are important OVOC
230 species emitted from vehicles. They show similar temporal variations as benzene and
231 toluene. However, concentrations of acetaldehyde and acetone were much lower than
232 the two aromatics after engine started. Compared to the concentrations at engine start-
233 up for the gasoline vehicle (the first cycle), concentrations of the VOCs are 3.0 to 40
234 times lower during the gasoline vehicle running at hot stabilized condition (the third
235 cycle). As shown in Fig. 1 for the diesel vehicle, enhanced emissions from cold start
236 are minor, which is different from the gasoline vehicle. The concentration of these
237 VOCs at engine start-up for the diesel vehicle are only 1.3 to 2.5 times higher than the
238 periods as the diesel vehicle running at hot stabilized condition. It indicates that the
239 impact of the engine start-up in diesel vehicles on emissions is much lower than
240 gasoline vehicles. It might be a combined effect of cold engine and operation
241 temperature of the after-treatment device. In contrast to the gasoline vehicle, we observe
242 higher concentrations of the two OVOC species than the two aromatics species from
243 the diesel vehicle. These higher OVOC concentrations in diesel vehicle exhausts are in
244 line with the observations of organic acids using the I-ToF-CIMS from the same
245 campaign (Li et al., 2021).

246 Based on the high time-resolution measurements of PTR-ToF-MS, we
247 determined emission factors of various VOC species from different vehicles. Fig. 2
248 shows the determined average mileage-based emission factors of benzene, toluene,
249 acetaldehyde, and acetone for various types of vehicles (also tabulated in the
250 Supplement table). In general, we observe a downward trend for emissions factors of
251 gasoline vehicles from China I to China VI emission standards for the four
252 representative VOC species. Emission factors of the four species for China VI vehicles
253 are 12 to 25 times lower than emissions for China I vehicles, indicating that newer
254 emission standards successfully reduced VOC emissions of gasoline vehicles. The



255 decline of emission factors for the four species with newer emission standards for diesel
256 vehicles are in the range of 1.1 to 7.4 times from China III to China V, compared to 4.5
257 to 5.4 times reduction from China III to China V for gasoline vehicles. Emission factors
258 of benzene and toluene from diesel vehicles are in the range of 0.8 to 7.4 $\text{mg}\cdot\text{km}^{-1}$ and
259 0.3 to 5.8 $\text{mg}\cdot\text{km}^{-1}$, which are comparable to emission factors from gasoline vehicles
260 with China IV to China VI emission standards. This is different from observations of
261 the two OVOC species (acetaldehyde and acetone), with much higher emission factors
262 from diesel vehicles (8.0 to 27.9 $\text{mg}\cdot\text{km}^{-1}$ for acetaldehyde and 0.8 to 10.0 $\text{mg}\cdot\text{km}^{-1}$ for
263 acetone) than almost all gasoline vehicles (a maximum of 3.9 $\text{mg}\cdot\text{km}^{-1}$ for acetaldehyde
264 and a maximum of 3.2 $\text{mg}\cdot\text{km}^{-1}$ for acetone). Higher emission factors from diesel
265 vehicles are also observed for many other common OVOC species, as shown in Fig. 3.
266 As the largest OVOCs emitted from gasoline vehicles ($4.6 \pm 5.1 \text{ mg}\cdot\text{km}^{-1}$), methanol is
267 found to be the only common OVOC species, with lower emission factors from diesel
268 vehicles than gasoline vehicles. The high emissions of OVOCs from diesel vehicles
269 may be related to combustion processes in diesel vehicles, with more excess air into
270 combustion cylinder resulting in higher oxygen contents and more oxidation processes
271 during fuel combustion (Pang et al., 2008; Qiao et al., 2012). Finally, the determined
272 emission factors of the four VOC species from LPG vehicles are much lower than both
273 gasoline and diesel vehicles.

274 **3.2 Analysis VOCs of PTR-ToF-MS mass spectra**

275 In addition to typical VOC species shown above, PTR-ToF-MS detected
276 abundant signals for a large number of ions. The determined average mileage-based
277 emission factors for all detected VOC species are shown as mass spectra in Fig. 4. VOC
278 species measured by PTR-ToF-MS were divided into groups according to chemical
279 formula, namely hydrocarbon species only containing C and H atoms (C_xH_y), OVOCs
280 ($\text{C}_x\text{H}_y\text{O}_z$), species containing nitrogen and/or sulfur atoms (N/S-containing), and some
281 other ions (others). We observe similar mass spectra of emission factors for gasoline
282 vehicles with different emission standards (Fig. S7). Highest emission factors from
283 gasoline vehicles (Fig. 4a) are detected as hydrocarbons, including C_6 to C_{10} aromatics.



284 A few OVOC species, namely methanol, ethanol, formaldehyde, acetaldehyde and
285 acetone, are also observed as the largest emissions. In contrast to gasoline vehicles, the
286 largest emissions from diesel vehicles were attributed to a few low-molecular-weight
287 OVOC species, including formaldehyde, acetaldehyde, formic acid, and acetic acid,
288 followed by a large number of hydrocarbon species. Comparison between the mass
289 spectra of gasoline and diesel vehicle emissions suggest that emissions from diesel
290 vehicles are more evenly distributed among different VOC species, as reflected by 50
291 and 140 species contributing more than 1% of the total emissions for gasoline and diesel
292 vehicles, respectively. As shown in Fig. 3b, many hydrocarbon ions in the range of m/z
293 150-200 still account for significant fractions of emissions from diesel vehicles,
294 whereas only one species in this m/z range contribute more than 1% of emissions from
295 gasoline vehicles. These results demonstrate that diesel vehicles emit more heavier
296 hydrocarbons than those from gasoline vehicles, which is consistent with observations
297 in previous studies (Gentner et al., 2012; Erickson et al., 2014). It should be noted that
298 the signals of $C_{16}H_{22}O_4H$ ($m/z=279$) were higher during the tests based on determined
299 emission factors. However, we suspect that it may be emitted artifacts from the
300 sampling or dilution system as it mainly showed higher signals in the latter period of
301 each test when sampling materials absorb more heat from vehicle exhausts (Fig. S8),
302 and thus it is not included in Fig. 3 (details in the Sect. 2 in the Supplement).

303 The scatterplot of carbon oxidation states (\overline{OS}_C) as a function of carbon number
304 (n_C) provides a framework for describing bulk chemical properties of organics (Kroll
305 et al., 2011). The details of \overline{OS}_C calculation is included in Sect. 3 in the Supplement.
306 The results from gasoline and diesel vehicles are compared in Fig. 5 (LPG vehicles are
307 shown in Fig. S9). It is apparent that ions with carbon oxidation states between -2.0 to
308 0 comprise main emissions for each carbon number for both gasoline and diesel
309 vehicles. It is interesting to observe that averaged \overline{OS}_C for $n_C > 6$ increase as the carbon
310 number decrease for both gasoline and diesel vehicles, whereas the opposite trends are
311 observed for $n_C < 5$. The averaged \overline{OS}_C in diesel vehicles for n_C between 1 and 5 are
312 significantly higher than those in gasoline vehicles, as the result of high emissions of
313 C_2 to C_5 low-molecular-weight OVOCs. Fig. 5c further shows that emission factors of



314 most VOC species from diesel vehicles were higher than gasoline vehicles, except a
315 number of species occupying in the right-bottom corner of the two-dimensional space.

316 The determined mass spectra of PTR-ToF-MS in terms of emission factor for
317 different types of vehicles can be used to explore the dependence of various VOC
318 emissions to different factors. Fig. 6a-b shows scatterplots of the average mileage-
319 based emission factors of VOCs between cold start and hot start for gasoline and diesel
320 vehicles, respectively. We observe strong correlation between emission factors from
321 cold start and hot start tests ($R=0.99$ and 0.92) and generally consistent ratios between
322 cold start and hot start for different types of VOC species for both gasoline and diesel
323 vehicles, indicating that variation behaviors are similar for different species and thus
324 chemical compositions of VOC emissions are comparable between different start
325 conditions. It is obvious that emission factors of VOCs during cold start are
326 significantly higher than those during hot start for gasoline vehicles (slope= 0.40),
327 whereas similar emissions factors between cold start and hot start are derived for diesel
328 vehicles (slope= 0.84). These results suggest that gasoline vehicles are more
329 significantly influenced by cold start, as the result of compositions in gasoline fuel are
330 more volatile than diesel fuel (US NRC, 1996). We further explore the effects of
331 emission standards to VOCs emission factors by comparing determined emission
332 factors between China I and China V for gasoline vehicle (Fig. 6c, also see China III
333 versus China V and China V versus China VI in Fig. S10) and between China III and
334 China V for LDDT (Fig. 6d, also see China III versus China V for MDDT and HDDT
335 in Fig. S10). Comparison of both gasoline and diesel vehicles demonstrate newer
336 emission standards successfully decreased VOC emissions. Based on the derived
337 slopes, we obtain VOCs emission factors reduced by a factor of 10 for gasoline
338 vehicles from China I to China V (a factor of 5 reduction from China III to China V
339 and a factor of 2.5 reduction for China V to China VI), and a factor of 2 reduction for
340 LDDT from China III to China V (a factor of 1.5 and 8 reduction for MDDT and
341 HDDT from China III to China V). The reduction ratio for gasoline vehicles from
342 China I to China V are generally similar for most VOC species, except that some
343 OVOC species with smaller reduction ratios. The reduction ratios for LDDT vehicles



344 from China III to China V show large variability for different species. The lowest
345 reduction ratios (a factor of ~ 2) are observed for the low-molecular weight OVOC
346 species associated with largest emissions, while the reduction ratios for hydrocarbons
347 and higher-molecular weight OVOCs are in the range of a factor of 10-100. These
348 results indicate the after-treatment device for diesel vehicles may effectively reduce
349 emissions of some heavier VOC species, though the after-treatment devices do not aim
350 for VOCs control.

351 **3.3 Non-target analysis for comparison between gasoline and diesel** 352 **vehicles**

353 As shown in the previous section, the analysis of PTR-ToF-MS mass spectra
354 provide rich information on understanding the influences of VOC emissions from
355 vehicles. This detailed information provided by the PTR-ToF-MS also offer an
356 opportunity to systematically compare emissions between gasoline and diesel vehicles.
357 The scatterplot of the determined average emission factors of various VOC species
358 between gasoline and diesel vehicles is shown in Fig. 7. Large difference of VOC
359 compositions emitted from gasoline and diesel vehicles are observed, as indicated by
360 the low correlation of the data points ($R=0.24$). A limited number of VOC species,
361 including C₆-C₁₀ aromatics and some N/S-containing species (e.g. C₇H₅N) are
362 associated with higher emission factors from gasoline vehicles, whereas the obtained
363 emission factors of most VOC species emitted from diesel vehicles are higher,
364 especially most OVOC species. For example, formic acid is found to be one of the
365 most significant emission species in diesel vehicles, with emission factors three orders
366 of magnitude higher than that of gasoline vehicles. In addition, emission factors of
367 HCN from gasoline vehicles are similar to those from diesel vehicles. These results
368 are consistent with the measurements using the I⁻ ToF-CIMS from the same campaign,
369 as shown in Li et al. (2021).

370 The scatterplot shown in Fig. 7 can also be expressed in terms of the determined
371 fuel-based emission factors between gasoline and diesel vehicles (Fig. S11). Generally,
372 similar variability is obtained except the determined slope of the data points, with



373 higher slopes determined from the scatterplot based on fuel-based emission factor
374 (0.19 versus 0.15). The difference between the slopes reflects the different average
375 mileage for the same weight of fuel between gasoline ($9.7 \text{ km}\cdot\text{kg}_{\text{fuel}}^{-1}$) and diesel
376 vehicles ($7.1 \text{ km}\cdot\text{kg}_{\text{fuel}}^{-1}$), as demonstrated for emission factors of CO_2 in Table S5.

377 From the comparison gasoline and diesel vehicles, we can also observe profound
378 differences in relative changes of emission factors for analogous compounds series. The
379 emission factors of C_6 - C_{10} aromatics are apparently higher for gasoline vehicles than
380 diesel vehicles, whereas emission factors for larger aromatics ($n_c > 11$) from diesel
381 vehicles start to exceed gasoline vehicles. This interesting behavior is the result of
382 different variations of emission factors for gasoline and diesel vehicles as carbon
383 number increases. As shown in Fig. 8, emission factors of aromatics from gasoline
384 vehicles start to rapidly decrease at $n_c = 10$ (a factor of 5 for each additional carbon for
385 C_{10} - C_{15}), while the emission factors of aromatic for diesel vehicles demonstrate a
386 relatively flat pattern between C_6 and C_{15} , only with significantly decrease for $n_c > 15$.
387 Based on Fig. 8, we determine that emissions of aromatics with $n_c \geq 10$ in gasoline and
388 diesel vehicles are account for 14% and 63% of total aromatic emissions, again suggest
389 the importance of heavier aromatics in emissions from diesel vehicles. It also highlights
390 that quantification of these heavier species by PTR-ToF-MS may be important in
391 characterization of vehicular exhausts, especially diesel vehicles.

392 In addition to aromatics, the relative changes of emission factors for carbonyls
393 with carbon number are apparently different between gasoline and diesel vehicles (Fig.
394 7 and Fig. 8b). Emission factors of carbonyls tend to decrease as carbon number
395 increase for both gasoline and diesel vehicles. The decrease magnitudes are observed
396 to be comparable from C_1 - C_6 carbonyls for gasoline (97.6%) and diesel vehicles
397 (97.4%). However, as $n_c > 6$, the decrease of carbonyl emissions factors for diesel
398 vehicles become smaller, result in larger emissions factors than gasoline vehicles for
399 this range of carbon number.

400 The above discussions demonstrate that emission characteristics of aromatics and
401 OVOCs are significantly different between gasoline and diesel vehicles. As the result,
402 the ratios of VOC pairs can be identified to distinguish emissions of gasoline and diesel



403 vehicles. Fig. 9 shows the scatterplots of four representative VOCs (benzene, C₁₄
404 aromatics, formaldehyde, and acetaldehyde) versus toluene based on the determined
405 emission factors. The data points for each VOCs pair clearly show distinct separation
406 between gasoline vehicles and diesel vehicles, with apparently higher slopes for diesel
407 vehicles than gasoline vehicles, as the result of much larger emission factors of toluene
408 from gasoline vehicles and lower emission factors of the four representative VOCs
409 from diesel vehicles. The benzene/toluene ratio in gasoline and diesel vehicle are
410 determined as 0.48 and 1.24 mg·mg⁻¹ (corresponding to 0.57 and 1.46 ppb·ppb⁻¹ that
411 are more widely used in ambient studies). The difference of benzene/toluene ratio
412 between gasoline and diesel vehicles has been reported in previous studies, and our
413 results are generally consistent with these previous results (Chan et al., 2002; Barletta
414 et al., 2005; Qiao et al., 2012; Kumar et al., 2020). Compared to benzene/toluene ratio,
415 the difference of C₁₄ aromatics/toluene ratio between gasoline and diesel vehicles are
416 more substantial (a factor of 3800). The remarkable larger emission factors of C₁₄
417 aromatics from diesel vehicles suggest that diesel vehicles can be a significant or even
418 predominated source for higher molecular aromatics. The enormous difference of C₁₄
419 aromatics/toluene ratio (and also other higher aromatics/toluene) between gasoline
420 and diesel vehicles indicate these ratios could potentially provide good indicators for
421 separation of gasoline and diesel vehicles in ambient or tunnel studies. Similar
422 discrepancies are observed for formaldehyde/toluene and acetaldehyde/toluene ratios
423 between gasoline and diesel vehicles. These ratios may not be able to be used as
424 indicators for distinguish gasoline and diesel vehicles in ambient studies, since
425 secondary sources may complicate the observed ratios in ambient air. However, these
426 results strongly suggest that diesel vehicles can be important in emissions of these
427 OVOC species, though the number of diesel vehicles are smaller than gasoline
428 vehicles in many countries, e.g. China and U.S (Wallington et al., 2013; Yao et al.,
429 2015; Huang et al., 2021).

430 3.4 OVOC fractions in VOC emissions

431 Emission factors of various VOC species measured by PTR-ToF-MS from



432 different vehicles are summarized in Fig. 10. As shown in Fig. 10a, the determined
433 average mileage-based emission factors of total VOC ions from diesel vehicles were
434 much higher than gasoline and LPG vehicles. Fig. 10b-d quantified the proportions of
435 different categories of ions measured by PTR-ToF-MS. The determined average
436 mileage-based emission factors of C_xH_y accounted for the largest fraction in gasoline
437 vehicles ($84\% \pm 5.9\%$), and lower fractions in diesel ($47\% \pm 16\%$) and LPG vehicles
438 ($32\% \pm 0.7\%$). OVOCs account for larger fractions in diesel ($49\% \pm 16\%$) and LPG
439 vehicles ($58\% \pm 3.7\%$), while they only account for $13\% \pm 6.1\%$ of emissions from
440 gasoline vehicles. The fractions of different OVOC groups generally demonstrate a
441 downward trend from $C_xH_yO_1$ to $C_xH_yO_{\geq 3}$, and OVOCs with more than two oxygen
442 atoms only occupy small percentages (0-7%) in vehicle exhausts, indicating low
443 emissions of these species.

444 Combined with measurements of other VOCs from canisters measured by GC-
445 MS/FID, the fractions of OVOCs in total VOC emissions can be determined for different
446 vehicles (details in Sect. 4 in the Supplement) (Fig. 11). OVOCs account for $7.7\% \pm$
447 6.2% of total VOC emissions for gasoline vehicles. The OVOC fractions for gasoline
448 vehicles are generally comparable for different emission standards and cold/hot start,
449 except somewhat higher fractions for China VI from hot start (Fig. S12). The OVOC
450 fractions obtained in this study for gasoline vehicles are generally consistent with
451 previous results (Cao et al., 2016; Wang et al., 2020b) (Fig. 11). Among these studies,
452 the OVOC fractions determined for gasoline with 10% ethanol (E10) (Roy et al., 2016)
453 ($22\% \pm 11\%$) are apparently higher. The fractions of OVOCs in total VOC emissions
454 for diesel vehicles are $77\% \pm 15\%$, $68\% \pm 15\%$, $73\% \pm 14\%$, and $40\% \pm 10\%$ for LDDT,
455 MDDT, HDDT, and bus, respectively. The variations of OVOC fractions with emission
456 standards are observed to be mixed among different types of diesel vehicles (Fig. S12).
457 The OVOC fractions from diesel vehicles are obviously higher than those in gasoline
458 vehicles, indicating the importance of OVOCs in VOC emissions for diesel vehicles.
459 Compared to previous studies (Tsai et al., 2012; Qiao et al., 2012; Cao et al., 2016; Mo
460 et al., 2016), determined OVOC fractions for diesel vehicles in this study are higher. If
461 only considering carbonyls among various types of OVOCs measured by PTR-ToF-MS,



462 the OVOC fractions determined in this study are more comparable with previous
463 studies (Fig. 11), since most previous studies only detected carbonyls among various
464 types of OVOCs. Finally, we determine that OVOCs account for $41\% \pm 8.6\%$ of total
465 VOC emissions for LPG vehicles, which is also higher than in one previous study
466 (Wang et al., 2020b) with only carbonyls and a few esters/alcohols included. These
467 results stress that the large number of OVOCs measured by PTR-ToF-MS are important
468 in characterization of VOC emissions from vehicles. It should be noted that the OVOC
469 fractions obtained here only reflect exhaust emissions. Evaporative emissions may be
470 associated with different fractions of various VOC groups, which may be more related
471 to fuel compositions (Rubin et al., 2006;Huang et al., 2021).

472 **4. Conclusions**

473 In this work, we conducted a chassis dynamometer study to measure VOC
474 emissions from gasoline, diesel, and LPG vehicles using PTR-ToF-MS along with other
475 offline and online measurement techniques. Using this dataset, we provide emission
476 factors of many VOCs from these three different types of vehicles associated with
477 various emission standards in China. Our results show that emission factors of VOCs
478 generally decrease with the increased stringency of emission standards for gasoline
479 vehicles, whereas variations of emission factors for diesel vehicles with emission
480 standards are more diverse. Mass spectra analysis of PTR-ToF-MS suggest that cold
481 start significantly influence VOCs emission of gasoline vehicles, while the influences
482 are smaller for diesel vehicles.

483 We observe large differences of VOC emissions between gasoline and diesel
484 vehicles based on PTR-ToF-MS measurements. Emission factors of most VOC species
485 from diesel vehicles were higher than gasoline vehicles, especially for most OVOCs
486 and heavier aromatics. The substantial larger emission factors of some OVOCs
487 emission factors for diesel vehicles indicate potentially dominant emissions of these
488 species from diesel vehicles among vehicular emissions. Our results suggest that VOC
489 pairs (e.g. C_{14} aromatics/toluene ratio) could potentially provide good indicators for
490 distinguishing emissions between gasoline and diesel vehicles.



491 Based on measurements of PTR-ToF-MS, C_xH_y ions account for the largest
492 fraction in gasoline vehicles ($84\% \pm 5.9\%$), whereas OVOC ions are the largest
493 contributor in the mass spectra of emissions from diesel ($49\% \pm 16\%$) and LPG vehicles
494 ($58\% \pm 3.7\%$). In the end, the fractions of OVOCs in total VOC emissions are
495 determined by combining hydrocarbons measurements from canister results and online
496 measurements of PTR-ToF-MS. We show that OVOCs contribute $7.7\% \pm 6.2\%$ of
497 gasoline vehicles of the total VOC emissions, while the fractions are significantly
498 higher for diesel vehicles (40-77%), highlighting the importance to detect these OVOC
499 species in diesel emissions.

500 This study shows significant contributions of OVOCs in VOC emissions from
501 various vehicles, especially diesel vehicles. As a consequence, vehicular emissions may
502 account for considerable proportions for primary emissions of these OVOCs in urban
503 regions. Emissions of many OVOC species are currently not fully represented in
504 emission inventories of VOCs, which may in turn affect the prediction ability of air
505 quality models in urban regions. In this study, OVOC species are mainly quantified
506 from PTR-ToF-MS measurements by taking into account all signals in the mass spectra,
507 which stress that the large number of OVOC species measured by PTR-ToF-MS are
508 important in characterization of VOC emissions from vehicles.

509 **Data availability**

510 Data are available from the authors upon request.

511 **Author contribution**

512 BY designed the research. ZBY, JYZ, BY, QES organized vehicle test
513 measurements. SHW, CHW, CMW, TGL, JPQ, QES, and MMZ contributed to data
514 collection. SHW performed the data analysis, with contributions from TGL, XJH, YBH,
515 XBL, and QES. SHW and BY prepared the manuscript with contributions from other
516 authors. All the authors reviewed the manuscript.

517 **Competing interests**

518 The authors declare that they have no known competing financial interests or
519 personal relationships that could have appeared to influence the work reported in this



520 paper.

521 **Acknowledgement**

522 This work was supported by the National Key R&D Plan of China (grant No.
523 2019YFE0106300, 2018YFC0213904), the National Natural Science Foundation of
524 China (grant No. 41877302, 42121004), Guangdong Natural Science Funds for
525 Distinguished Young Scholar (grant No. 2018B030306037), and Guangdong
526 Innovative and Entrepreneurial Research Team Program (grant No. 2016ZT06N263).
527 This work was also supported by Special Fund Project for Science and Technology
528 Innovation Strategy of Guangdong Province (Grant No.2019B121205004). TK and
529 MG were supported by OEAD grant CN 05/2020.

530



531 **References**

- 532 Permissible Exposure Levels for Selected Military Fuel Vapors, The National
533 Academies Press, Washington, DC, 1996.
- 534 Barletta, B., Meinardi, S., Sherwood Rowland, F., Chan, C.-Y., Wang, X., Zou, S., Yin
535 Chan, L., and Blake, D. R.: Volatile organic compounds in 43 Chinese cities,
536 Atmospheric Environment, 39, 5979-5990, 10.1016/j.atmosenv.2005.06.029, 2005.
- 537 Cao, X., Yao, Z., Shen, X., Ye, Y., and Jiang, X.: On-road emission characteristics of
538 VOCs from light-duty gasoline vehicles in Beijing, China, Atmospheric Environment,
539 124, 146-155, 10.1016/j.atmosenv.2015.06.019, 2016.
- 540 Cappellin, L., Karl, T., Probst, M., Ismailova, O., Winkler, P. M., Soukoulis, C., Aprea,
541 E., Mark, T. D., Gasperi, F., and Biasioli, F.: On quantitative determination of volatile
542 organic compound concentrations using proton transfer reaction time-of-flight mass
543 spectrometry, Environmental Science & Technology, 46, 2283-2290,
544 10.1021/es203985t, 2012.
- 545 Chan, C. Y., Chan, L. Y., Wang, X. M., Liu, Y. M., Lee, S. C., Zou, S. C., Sheng, G. Y.,
546 and Fu, J. M.: Volatile organic compounds in roadside microenvironments of
547 metropolitan Hong Kong, Atmospheric Environment, 36, 2039-2047,
548 [https://doi.org/10.1016/S1352-2310\(02\)00097-3](https://doi.org/10.1016/S1352-2310(02)00097-3), 2002.
- 549 Cui, L., Wang, X. L., Ho, K. F., Gao, Y., Liu, C., Hang Ho, S. S., Li, H. W., Lee, S. C.,
550 Wang, X. M., Jiang, B. Q., Huang, Y., Chow, J. C., Watson, J. G., and Chen, L.-W.:
551 Decrease of VOC emissions from vehicular emissions in Hong Kong from 2003 to 2015:
552 Results from a tunnel study, Atmospheric Environment, 177, 64-74,
553 10.1016/j.atmosenv.2018.01.020, 2018.
- 554 Drozd, G. T., Zhao, Y., Saliba, G., Frodin, B., Maddox, C., Weber, R. J., Chang, M. O.,
555 Maldonado, H., Sardar, S., Robinson, A. L., and Goldstein, A. H.: Time Resolved
556 Measurements of Speciated Tailpipe Emissions from Motor Vehicles: Trends with
557 Emission Control Technology, Cold Start Effects, and Speciation, Environmental
558 Science & Technology, 50, 13592-13599, 10.1021/acs.est.6b04513, 2016.
- 559 Erickson, M. H., Gueneron, M., and Jobson, B. T.: Measuring long chain alkanes in
560 diesel engine exhaust by thermal desorption PTR-MS, Atmospheric Measurement
561 Techniques, 7, 225-239, 10.5194/amt-7-225-2014, 2014.
- 562 Gentner, D. R., Isaacman, G., Worton, D. R., Chan, A. W., Dallmann, T. R., Davis, L.,
563 Liu, S., Day, D. A., Russell, L. M., Wilson, K. R., Weber, R., Guha, A., Harley, R. A.,
564 and Goldstein, A. H.: Elucidating secondary organic aerosol from diesel and gasoline
565 vehicles through detailed characterization of organic carbon emissions, Proc Natl Acad
566 Sci U S A, 109, 18318-18323, 10.1073/pnas.1212272109, 2012.
- 567 Guo, H., Zou, S. C., Tsai, W. Y., Chan, L. Y., and Blake, D. R.: Emission characteristics
568 of nonmethane hydrocarbons from private cars and taxis at different driving speeds in
569 Hong Kong, Atmospheric Environment, 45, 2711-2721,
570 10.1016/j.atmosenv.2011.02.053, 2011.
- 571 Han, C., Liu, R., Luo, H., Li, G., Ma, S., Chen, J., and An, T.: Pollution profiles of
572 volatile organic compounds from different urban functional areas in Guangzhou China



573 based on GC/MS and PTR-TOF-MS: Atmospheric environmental implications,
574 *Atmospheric Environment*, 214, 10.1016/j.atmosenv.2019.116843, 2019.

575 He, X., Yuan, B., Wu, C., Wang, S., Wang, C., Huangfu, Y., Qi, J., Ma, N., Xu, W.,
576 Wang, M., Chen, W., Su, H., Cheng, Y., and Shao, M.: Volatile organic compounds in
577 wintertime North China Plain: Insights from measurements of proton transfer reaction
578 time-of-flight mass spectrometer (PTR-ToF-MS), *Journal of Environmental Sciences*,
579 10.1016/j.jes.2021.08.010, 2022.

580 Huang, J., Yuan, Z., Duan, Y., Liu, D., Fu, Q., Liang, G., Li, F., and Huang, X.:
581 Quantification of temperature dependence of vehicle evaporative volatile organic
582 compound emissions from different fuel types in China, *Sci Total Environ*, 813, 152661,
583 10.1016/j.scitotenv.2021.152661, 2021.

584 http://e.jmrb.com/m/2008/11/17/10/m_182226.shtml, Access on 2009-12-10, 2008.

585 Kansal, A.: Sources and reactivity of NMHCs and VOCs in the atmosphere: a review,
586 *J Hazard Mater*, 166, 17-26, 10.1016/j.jhazmat.2008.11.048, 2009.

587 Koss, A. R., Sekimoto, K., Gilman, J. B., Selimovic, V., Coggon, M. M., Zarzana, K.
588 J., Yuan, B., Lerner, B. M., Brown, S. S., Jimenez, J. L., Krechmer, J., Roberts, J. M.,
589 Warneke, C., Yokelson, R. J., and de Gouw, J.: Non-methane organic gas emissions
590 from biomass burning: identification, quantification, and emission factors from PTR-
591 ToF during the FIREX 2016 laboratory experiment, *Atmospheric Chemistry and
592 Physics*, 18, 3299-3319, 10.5194/acp-18-3299-2018, 2018.

593 Kroll, J. H., Donahue, N. M., Jimenez, J. L., Kessler, S. H., Canagaratna, M. R., Wilson,
594 K. R., Altieri, K. E., Mazzoleni, L. R., Wozniak, A. S., Bluhm, H., Mysak, E. R., Smith,
595 J. D., Kolb, C. E., and Worsnop, D. R.: Carbon oxidation state as a metric for describing
596 the chemistry of atmospheric organic aerosol, *Nat Chem*, 3, 133-139,
597 10.1038/nchem.948, 2011.

598 Kumar, A., Sinha, V., Shabin, M., Hakkim, H., Bonsang, B., and Gros, V.: Non-methane
599 hydrocarbon (NMHC) fingerprints of major urban and agricultural emission sources for
600 use in source apportionment studies, *Atmospheric Chemistry and Physics*, 20, 12133-
601 12152, 10.5194/acp-20-12133-2020, 2020.

602 Laurikko, J.: Ambient temperature effect on automotive exhaust emissions: FTP and
603 ECE test cycle responses, *The Science of Environment*, 169, 195-204, 1995.

604 Li, B., Ho, S. S. H., Xue, Y., Huang, Y., Wang, L., Cheng, Y., Dai, W., Zhong, H., Cao,
605 J., and Lee, S.: Characterizations of volatile organic compounds (VOCs) from vehicular
606 emissions at roadside environment: The first comprehensive study in Northwestern
607 China, *Atmospheric Environment*, 161, 1-12, 10.1016/j.atmosenv.2017.04.029, 2017.

608 Li, T., Wang, Z., Yuan, B., Ye, C., Lin, Y., Wang, S., Sha, Q. e., Yuan, Z., Zheng, J., and
609 Shao, M.: Emissions of carboxylic acids, hydrogen cyanide (HCN) and isocyanic acid
610 (HNCO) from vehicle exhaust, *Atmospheric Environment*,
611 10.1016/j.atmosenv.2021.118218, 2021.

612 Li, X., Wu, Y., Yao, X., Zhang, S., Zhou, Y., and Fu, L.: Evaluation of the environmental
613 benefits of the enhanced vehicle inspection /maintenance program based on the short
614 transient loaded mode in Guangzhou (in Chinese), *Acta Scientiae Circumstantiae*, 32(1),
615 101-108, 10.13671/j.hjkxxb.2012.01.009, 2012.



- 616 Liao, S., Zhang, J., Yu, F., Zhu, M., Liu, J., Ou, J., Dong, H., Sha, Q., Zhong, Z., Xie,
617 Y., Luo, H., Zhang, L., and Zheng, J.: High Gaseous Nitrous Acid (HONO) Emissions
618 from Light-Duty Diesel Vehicles, *Environ Sci Technol*, 55, 200-208,
619 10.1021/acs.est.0c05599, 2021.
- 620 Liu, Y., Shao, M., Fu, L., Lu, S., Zeng, L., and Tang, D.: Source profiles of volatile
621 organic compounds (VOCs) measured in China: Part I, *Atmospheric Environment*, 42,
622 6247-6260, 10.1016/j.atmosenv.2008.01.070, 2008.
- 623 Liu, Y., Li, Y., Yuan, Z., Wang, H., Sha, Q., Lou, S., Liu, Y., Hao, Y., Duan, L., Ye, P.,
624 Zheng, J., Yuan, B., and Shao, M.: Identification of two main origins of intermediate-
625 volatility organic compound emissions from vehicles in China through two-phase
626 simultaneous characterization, *Environ Pollut*, 281, 117020,
627 10.1016/j.envpol.2021.117020, 2021.
- 628 Ly, B. T., Kajii, Y., Nguyen, T. Y., Shoji, K., Van, D. A., Do, T. N., Nghiem, T. D., and
629 Sakamoto, Y.: Characteristics of roadside volatile organic compounds in an urban area
630 dominated by gasoline vehicles, a case study in Hanoi, *Chemosphere*, 254, 126749,
631 10.1016/j.chemosphere.2020.126749, 2020.
- 632 May, A. A., Nguyen, N. T., Presto, A. A., Gordon, T. D., Lipsky, E. M., Karve, M.,
633 Gutierrez, A., Robertson, W. H., Zhang, M., Brandow, C., Chang, O., Chen, S., Cicero-
634 Fernandez, P., Dinkins, L., Fuentes, M., Huang, S.-M., Ling, R., Long, J., Maddox, C.,
635 Massetti, J., McCauley, E., Miguel, A., Na, K., Ong, R., Pang, Y., Rieger, P., Sax, T.,
636 Truong, T., Vo, T., Chattopadhyay, S., Maldonado, H., Maricq, M. M., and Robinson,
637 A. L.: Gas- and particle-phase primary emissions from in-use, on-road gasoline and
638 diesel vehicles, *Atmospheric Environment*, 88, 247-260,
639 10.1016/j.atmosenv.2014.01.046, 2014.
- 640 China Mobile Source Environmental Management Annual Report:
641 <http://www.mee.gov.cn/hjzl/sthjzk/ydyhjgl/201909/P020190905586230826402.pdf>,
642 2019.
- 643 Mo, Z., Shao, M., and Lu, S.: Compilation of a source profile database for hydrocarbon
644 and OVOC emissions in China, *Atmospheric Environment*, 143, 209-217,
645 10.1016/j.atmosenv.2016.08.025, 2016.
- 646 Ou, J., Zheng, J., Li, R., Huang, X., Zhong, Z., Zhong, L., and Lin, H.: Speciated OVOC
647 and VOC emission inventories and their implications for reactivity-based ozone control
648 strategy in the Pearl River Delta region, China, *Sci Total Environ*, 530-531, 393-402,
649 10.1016/j.scitotenv.2015.05.062, 2015.
- 650 Pang, X., Mu, Y., Yuan, J., and He, H.: Carbonyls emission from ethanol-blended
651 gasoline and biodiesel-ethanol-diesel used in engines, *Atmospheric Environment*, 42,
652 1349-1358, 10.1016/j.atmosenv.2007.10.075, 2008.
- 653 Parrish, D. D., Kuster, W. C., Shao, M., Yokouchi, Y., Kondo, Y., Goldan, P. D., de
654 Gouw, J. A., Koike, M., and Shirai, T.: Comparison of air pollutant emissions among
655 mega-cities, *Atmospheric Environment*, 43, 6435-6441,
656 10.1016/j.atmosenv.2009.06.024, 2009.
- 657 Qi, L., Liu, H., Shen, X., Fu, M., Huang, F., Man, H., Deng, F., Shaikh, A. A., Wang,
658 X., Dong, R., Song, C., and He, K.: Intermediate-Volatility Organic Compound



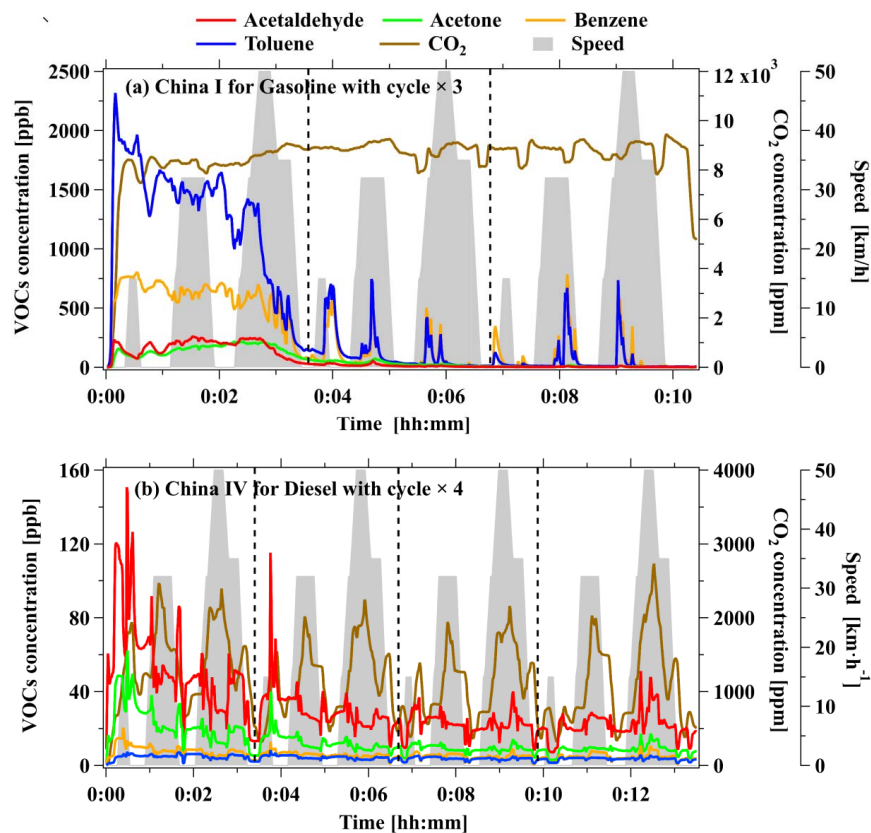
- 659 Emissions from Nonroad Construction Machinery under Different Operation Modes,
660 Environ Sci Technol, 53, 13832-13840, 10.1021/acs.est.9b01316, 2019.
- 661 Qiao, Y. Z., Wang, H. L., Huang, C., Chen, C. H., and Huang, H. Y.: Source profile and
662 chemical reactivity of volatile organic compounds from vehicle exhaust(in chinese),
663 Environmental Science, 33, 1071-1079, 2012.
- 664 Roy, A., Sonntag, D., Cook, R., Yanca, C., Schenk, C., and Choi, Y.: Effect of Ambient
665 Temperature on Total Organic Gas Speciation Profiles from Light-Duty Gasoline
666 Vehicle Exhaust, Environmental Science & Technology, 50, 6565-6573,
667 10.1021/acs.est.6b01081, 2016.
- 668 Rubin, J. I., Kean, A. J., Harley, R. A., Millet, D. B., and Goldstein, A. H.: Temperature
669 dependence of volatile organic compound evaporative emissions from motor vehicles,
670 Journal of Geophysical Research: Atmospheres, 111,
671 <https://doi.org/10.1029/2005JD006458>, 2006.
- 672 Schauer, J. J., Kleeman, M. J., Cass, G. R., and Simoneit, B. R., T.: Measurement of
673 Emissions from Air Pollution Sources. 2. C₁ through C₃₀ Organic Compounds from
674 Medium Duty Diesel Trucks, Environmental Science & Technology, 33, 1578-1587,
675 1999.
- 676 Seinfeld, J. H., and Pandis, S. N.: Atmospheric chemistry and physics: from air
677 pollution to climate change, John Wiley & Sons, Inc., Hoboken, 2006.
- 678 Sekimoto, K., Li, S.-M., Yuan, B., Koss, A., Coggon, M., Warneke, C., and de Gouw,
679 J.: Calculation of the sensitivity of proton-transfer-reaction mass spectrometry (PTR-
680 MS) for organic trace gases using molecular properties, International Journal of Mass
681 Spectrometry, 421, 71-94, 10.1016/j.ijms.2017.04.006, 2017.
- 682 Shao, M., Zhang, Y., Zeng, L., Tang, X., Zhang, J., Zhong, L., and Wang, B.: Ground-
683 level ozone in the Pearl River Delta and the roles of VOC and NO_x in its production,
684 Journal of Environmental Management, 90, 512-518, 10.1016/j.jenvman.2007.12.008,
685 2009.
- 686 Song, C., Liu, Y., Sun, L., Zhang, Q., and Mao, H.: Emissions of volatile organic
687 compounds (VOCs) from gasoline- and liquified natural gas (LNG)-fueled vehicles in
688 tunnel studies, Atmospheric Environment, 234, 10.1016/j.atmosenv.2020.117626, 2020.
- 689 Stark, H., Yatavelli, R. L. N., Thompson, S. L., Kimmel, J. R., Cubison, M. J., Chhabra,
690 P. S., Canagaratna, M. R., Jayne, J. T., Worsnop, D. R., and Jimenez, J. L.: Methods to
691 extract molecular and bulk chemical information from series of complex mass spectra
692 with limited mass resolution, International Journal of Mass Spectrometry, 389, 26-38,
693 10.1016/j.ijms.2015.08.011, 2015.
- 694 Sulzer, P., Hartungen, E., Hanel, G., Feil, S., Winkler, K., Mutschlechner, P., Haidacher,
695 S., Schottkowsky, R., Gansch, D., Seehauser, H., Striednig, M., Jürschik, S., Breiev, K.,
696 Lanza, M., Herbig, J., Märk, L., Märk, T. D., and Jordan, A.: A Proton Transfer
697 Reaction-Quadrupole interface Time-Of-Flight Mass Spectrometer (PTR-QiTOF):
698 High speed due to extreme sensitivity, International Journal of Mass Spectrometry, 368,
699 1-5, 10.1016/j.ijms.2014.05.004, 2014.
- 700 Sun, W., Shao, M., Granier, C., Liu, Y., Ye, C. S., and Zheng, J. Y.: Long-Term Trends
701 of Anthropogenic SO₂, NO_x, CO, and NMVOCs Emissions in China, Earth's Future,
702 6, 1112-1133, 10.1029/2018ef000822, 2018.



- 703 Tsai, J.-H., Chang, S.-Y., and Chiang, H.-L.: Volatile organic compounds from the
704 exhaust of light-duty diesel vehicles, *Atmospheric Environment*, 61, 499-506,
705 10.1016/j.atmosenv.2012.07.078, 2012.
- 706 Wallington, T. J., Lambert, C. K., and Ruona, W. C.: Diesel vehicles and sustainable
707 mobility in the U.S, *Energy Policy*, 54, 47-53, 10.1016/j.enpol.2011.11.068, 2013.
- 708 Wang, C., Yuan, B., Wu, C., Wang, S., Qi, J., Wang, B., Wang, Z., Hu, W., Chen, W.,
709 Ye, C., Wang, W., Sun, Y., Wang, C., Huang, S., Song, W., Wang, X., Yang, S., Zhang,
710 S., Xu, W., Ma, N., Zhang, Z., Jiang, B., Su, H., Cheng, Y., Wang, X., and Shao, M.:
711 Measurements of higher alkanes using NO⁺ chemical ionization in PTR-ToF-MS:
712 important contributions of higher alkanes to secondary organic aerosols in China,
713 *Atmospheric Chemistry and Physics*, 20, 14123-14138, 10.5194/acp-20-14123-2020,
714 2020a.
- 715 Wang, H., L., Jing, S., A., Lou, S., R., Hu, Q., Y., Li, L., Tao, S., K., Huang, C., Qiao,
716 L., P., and Chen, C., H.: Volatile organic compounds (VOCs) source profiles of on-
717 road vehicle emissions in China, *Sci Total Environ*, 607-608, 253-261,
718 10.1016/j.scitotenv.2017.07.001, 2017.
- 719 Wang, J., Jin, L., Gao, J., Shi, J., Zhao, Y., Liu, S., Jin, T., Bai, Z., and Wu, C. Y.:
720 Investigation of speciated VOC in gasoline vehicular exhaust under ECE and EUDC
721 test cycles, *Sci Total Environ*, 445-446, 110-116, 10.1016/j.scitotenv.2012.12.044, 2013.
- 722 Wang, M., Li, S., Zhu, R., Zhang, R., Zu, L., Wang, Y., and Bao, X.: On-road tailpipe
723 emission characteristics and ozone formation potentials of VOCs from gasoline, diesel
724 and liquefied petroleum gas fueled vehicles, *Atmospheric Environment*,
725 10.1016/j.atmosenv.2020.117294, 2020b.
- 726 Wang, Z., Yuan, B., Ye, C., Roberts, J., Wisthaler, A., Lin, Y., Li, T., Wu, C., Peng, Y.,
727 Wang, C., Wang, S., Yang, S., Wang, B., Qi, J., Wang, C., Song, W., Hu, W., Wang, X.,
728 Xu, W., Ma, N., Kuang, Y., Tao, J., Zhang, Z., Su, H., Cheng, Y., Wang, X., and Shao,
729 M.: High Concentrations of Atmospheric Isocyanic Acid (HNCO) Produced from
730 Secondary Sources in China, *Environmental Science & Technology*,
731 10.1021/acs.est.0c02843, 2020c.
- 732 Wu, C., Wang, C., Wang, S., Wang, W., Yuan, B., Qi, J., Wang, B., Wang, H., Wang, C.,
733 Song, W., Wang, X., Hu, W., Lou, S., Ye, C., Peng, Y., Wang, Z., Huangfu, Y., Xie, Y.,
734 Zhu, M., Zheng, J., Wang, X., Jiang, B., Zhang, Z., and Shao, M.: Measurement report:
735 Important contributions of oxygenated compounds to emissions and chemistry of
736 volatile organic compounds in urban air, *Atmospheric Chemistry and Physics*, 20,
737 14769-14785, 10.5194/acp-20-14769-2020, 2020.
- 738 Wu, R., Bo, Y., Li, J., Li, L., Li, Y., and Xie, S.: Method to establish the emission
739 inventory of anthropogenic volatile organic compounds in China and its application in
740 the period 2008–2012, *Atmospheric Environment*, 127, 244-254,
741 10.1016/j.atmosenv.2015.12.015, 2016.
- 742 Wu, Y., Zhang, S., Hao, J., Liu, H., Wu, X., Hu, J., Walsh, M. P., Wallington, T. J.,
743 Zhang, K. M., and Stevanovic, S.: On-road vehicle emissions and their control in China:
744 A review and outlook, *Sci Total Environ*, 574, 332-349,
745 10.1016/j.scitotenv.2016.09.040, 2017.



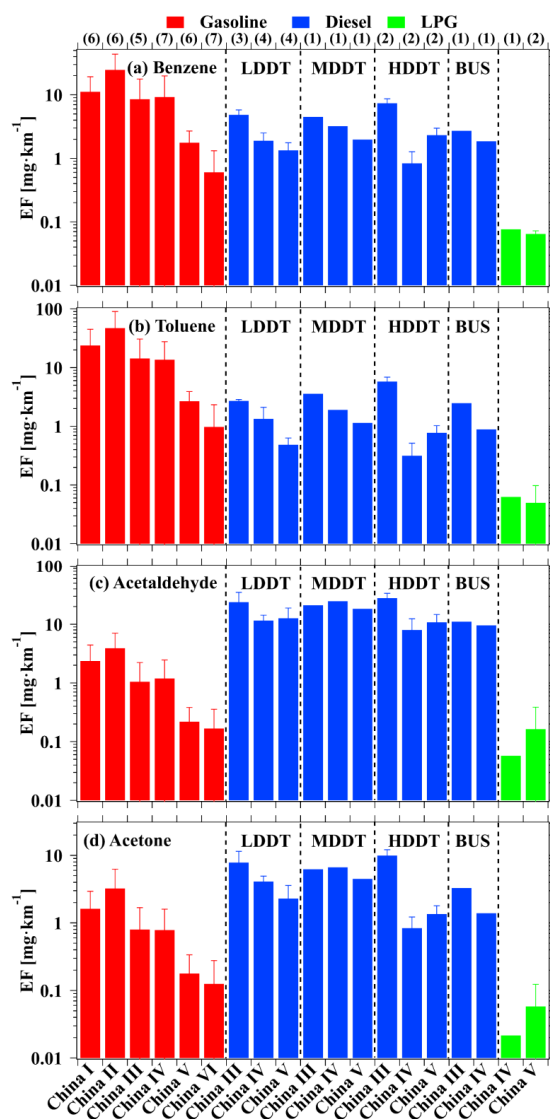
- 746 Yang, W., Zhang, Q., Wang, J., Zhou, C., Zhang, Y., and Pan, Z.: Emission
747 characteristics and ozone formation potentials of VOCs from gasoline passenger cars
748 at different driving modes, *Atmospheric Pollution Research*, 9, 804-813,
749 10.1016/j.apr.2018.01.002, 2018.
- 750 Yao, S., Liu, Z., and Qi, Z.: Test System for Exhaust Pollutants from Light-duty
751 Gasoline Vehicle under Short Transient Driving Cycle (in Chinese), *Shanghai*
752 *Environmental Sciences*, 10, 722-728, 2003.
- 753 Yao, Z., Shen, X., Ye, Y., Cao, X., Jiang, X., Zhang, Y., and He, K.: On-road emission
754 characteristics of VOCs from diesel trucks in Beijing, China, *Atmospheric Environment*,
755 103, 87-93, 10.1016/j.atmosenv.2014.12.028, 2015.
- 756 Ye, C., Yuan, B., Lin, Y., Wang, Z., Hu, W., Li, T., Chen, W., Wu, C., Wang, C., Huang,
757 S., Qi, J., Wang, B., Wang, C., Song, W., Wang, X., Zheng, E., Krechmer, J. E., Ye, P.,
758 Zhang, Z., Wang, X., Worsnop, D. R., and Shao, M.: Chemical characterization of
759 oxygenated organic compounds in the gas phase and particle phase using iodide CIMS
760 with FIGAERO in urban air, *Atmospheric Chemistry and Physics*, 21, 8455-8478,
761 10.5194/acp-21-8455-2021, 2021.
- 762 Yuan, B., Koss, A. R., Warneke, C., Coggon, M., Sekimoto, K., and de Gouw, J. A.:
763 Proton-Transfer-Reaction Mass Spectrometry: Applications in Atmospheric Sciences,
764 *Chemical Reviews*, 117, 13187-13229, 10.1021/acs.chemrev.7b00325, 2017.
- 765 Zavala, M., Herndon, S. C., Slott, R. S., Dunlea, E. J., Marr, L. C., Shorter, J. H.,
766 Zahniser, M., Knighton, W. B., Rogers, T. M., Kolb, C. E., Molina, L. T., and Molina,
767 M. J.: Characterization of on-road vehicle emissions in the Mexico City Metropolitan
768 Area using a mobile laboratory in chase and fleet average measurement modes during
769 the MCMA-2003 field campaign, *Atmospheric Chemistry and Physics*, 6, 5129-5142,
770 10.5194/acp-6-5129-2006, 2006.
- 771 Zavala, M., Herndon, S. C., Wood, E. C., Jayne, J. T., Nelson, D. D., Trimborn, A. M.,
772 Dunlea, E., Knighton, W. B., Mendoza, A., Allen, D. T., Kolb, C. E., Molina, M. J., and
773 Molina, L. T.: Comparison of emissions from on-road sources using a mobile laboratory
774 under various driving and operational sampling modes, *Atmospheric Chemistry and*
775 *Physics*, 9, 1-14, 10.5194/acp-9-1-2009, 2009.
- 776 Zhang, Q., Wu, L., Fang, X., Liu, M., Zhang, J., Shao, M., Lu, S., and Mao, H.:
777 Emission factors of volatile organic compounds (VOCs) based on the detailed vehicle
778 classification in a tunnel study, *Sci Total Environ*, 624, 878-886,
779 10.1016/j.scitotenv.2017.12.171, 2018.
- 780 Zhu, M., Dong, H., Yu, F., Liao, S., Xie, Y., Liu, J., Sha, Q., Zhong, Z., Zeng, L., and
781 Zheng, J.: A New Portable Instrument for Online Measurements of Formaldehyde:
782 From Ambient to Mobile Emission Sources, *Environmental Science & Technology*
783 *Letters*, 7, 292-297, 10.1021/acs.estlett.0c00169, 2020.
- 784 Ziemann, P. J., and Atkinson, R.: Kinetics, products, and mechanisms of secondary
785 organic aerosol formation, *Chem Soc Rev*, 41, 6582-6605, 10.1039/c2cs35122f, 2012.
- 786
787



788

789 **Figure 1.** Real-time concentrations of acetaldehyde, acetone, benzene, toluene, and
790 CO₂ for (a) a gasoline vehicle with emission standard of China I and (b) a light-duty
791 diesel vehicle with emission standard of China IV. The two vehicles were both cold
792 started. The gray shadows represent the speed of the vehicles on the chassis
793 dynamometer.

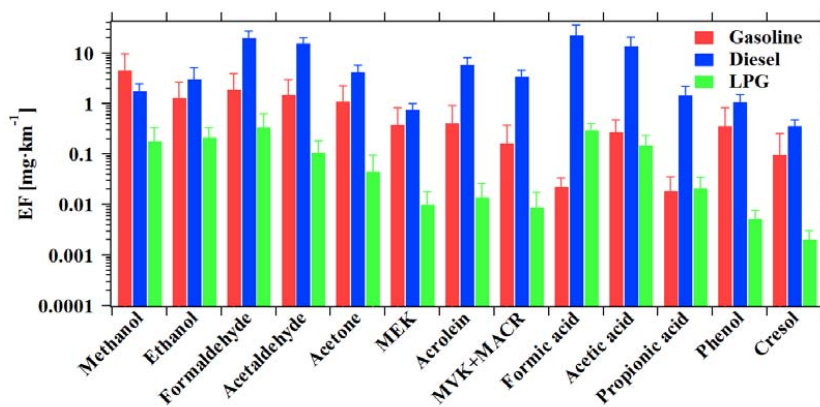
794



795

796 **Figure 2.** The determined average mileage-based emission factors ($\text{mg}\cdot\text{km}^{-1}$) for (a)
 797 benzene, (b) toluene, (c) acetaldehyde, and (d) acetone for vehicles with different
 798 emission standards. The numbers above the top axis represent the number of all
 799 experiments (including multiple measurements for individual test vehicle) for each
 800 emission standard. Error bars represent standard deviations of emission factors for the
 801 specific emission standard.

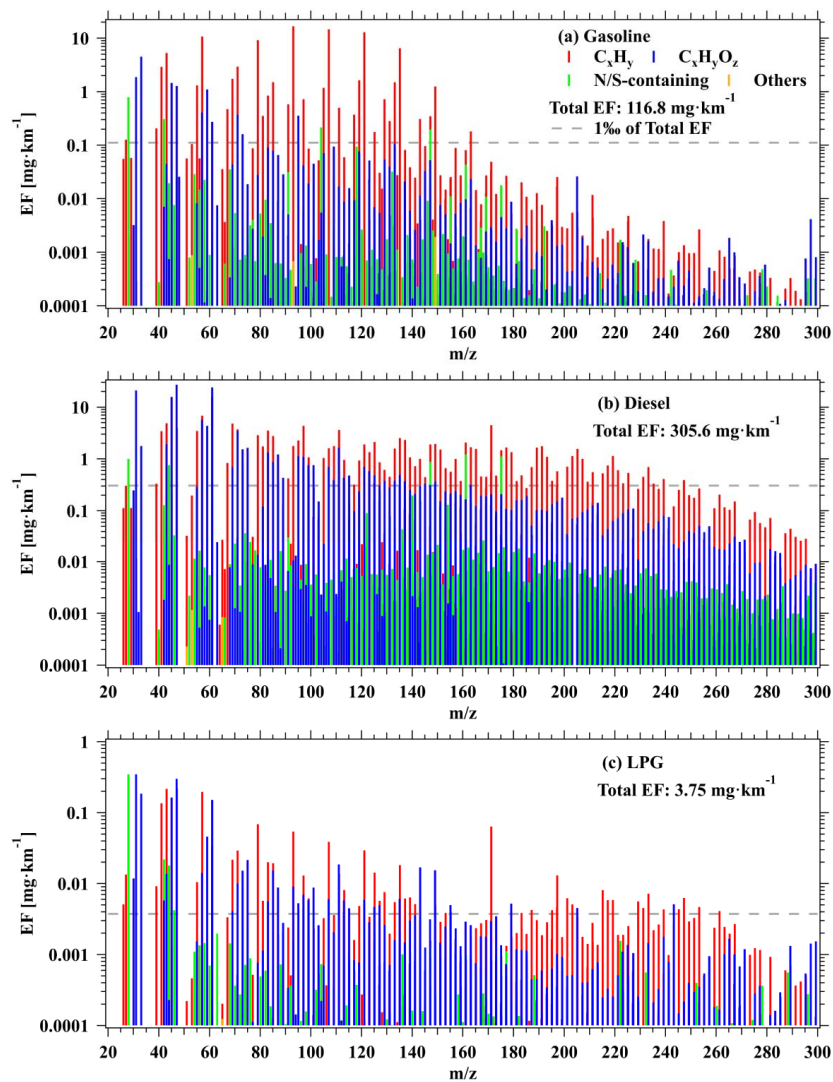
802



803

804 **Figure 3.** The determined emission factors of representative OVOC species from
805 different types of vehicles. Error bars represent standard deviations of the emission
806 factors for the VOCs.

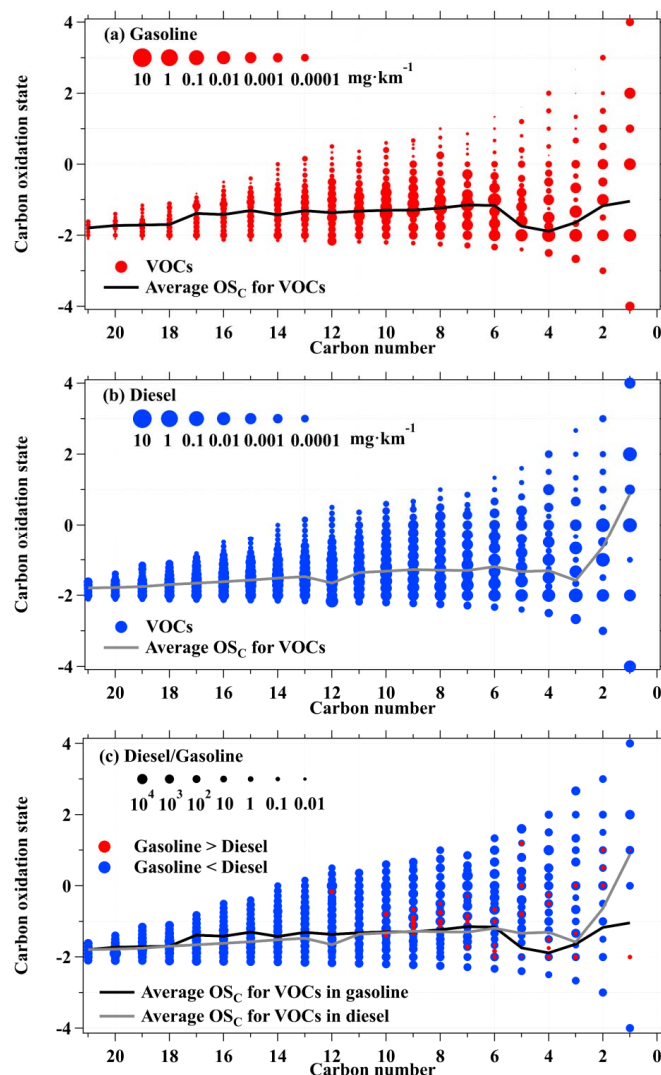
807



808

809 **Figure 4.** The determined average mileage-based emission factors of VOC species
810 measured by PTR-ToF-MS from (a) gasoline, (b) diesel, and (c) LPG vehicles. The
811 gray dashed lines represent 1% of total VOCs emission factors.

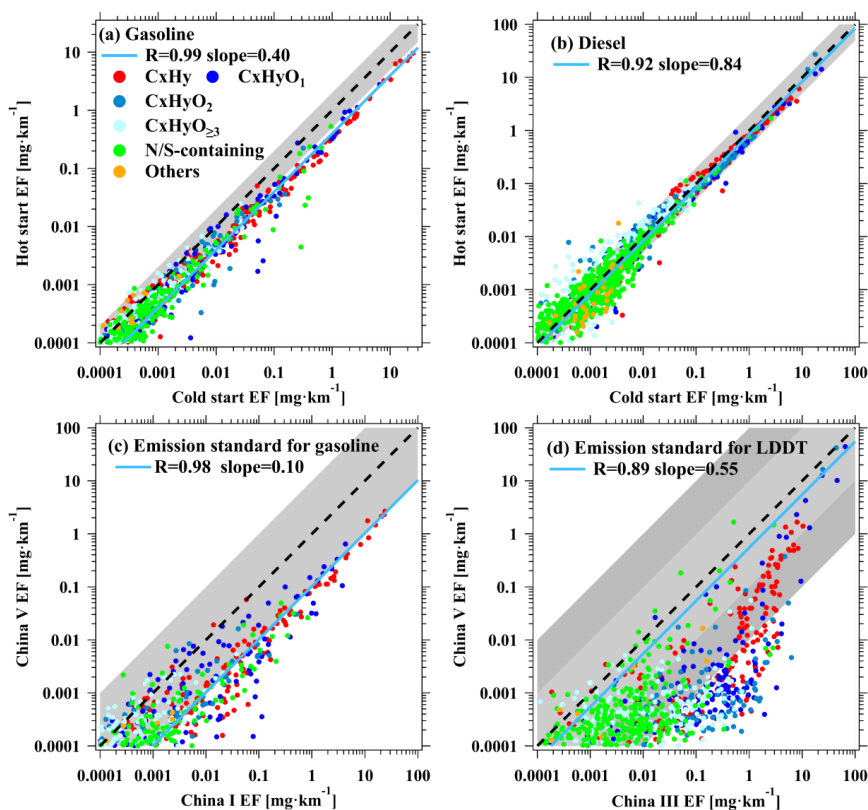
812



813

814 **Figure 5.** The two-dimensional space of $\overline{OS}_C - n_C$ with data points sized coded using
 815 emission factors of VOC species from (a) gasoline and (b) diesel vehicles, and (c) the
 816 ratio of emission factors of diesel vehicle relative to gasoline vehicle. The black and
 817 gray lines are the average \overline{OS}_C of each carbon number for VOC species in gasoline
 818 and diesel vehicles, respectively.

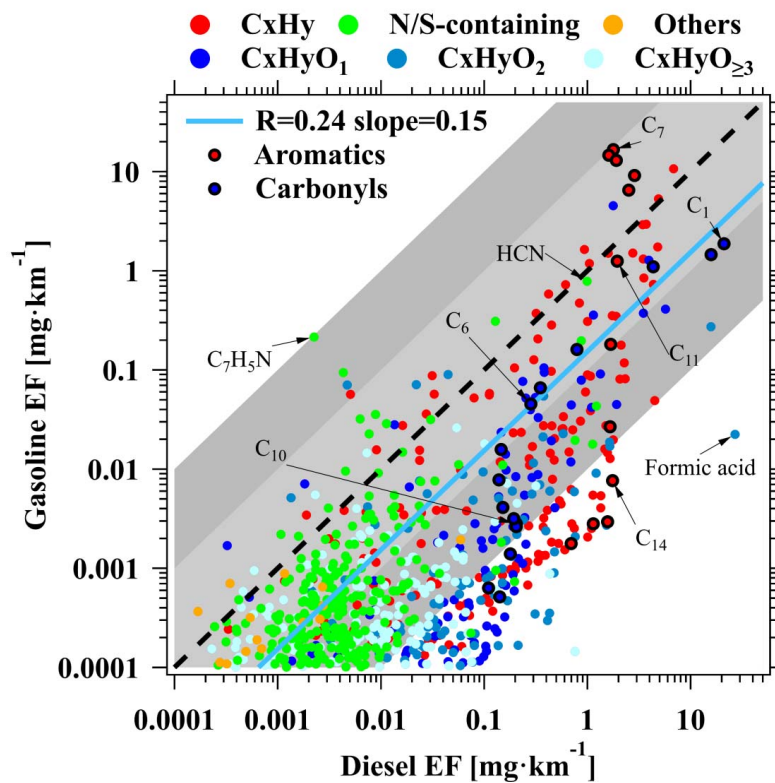
819



820

821 **Figure 6.** Scatterplots of VOCs emission factors between cold start and hot start for
822 gasoline (a) and diesel vehicles (b). Scatterplots of VOCs emission factors between
823 China I and China V emission standard for gasoline vehicles (c) and between China III
824 and China V emission standard for diesel vehicles (d). Each data point indicates a VOC
825 species measured by PTR-ToF-MS. The blue lines are the fitted results for all data
826 points. The black dashed lines represent 1:1 ratio, and the shaded areas represent ratios
827 of a factor of 2 in (a) and (b), and a factor of 10 and 100 in (c) and (d).

828



829

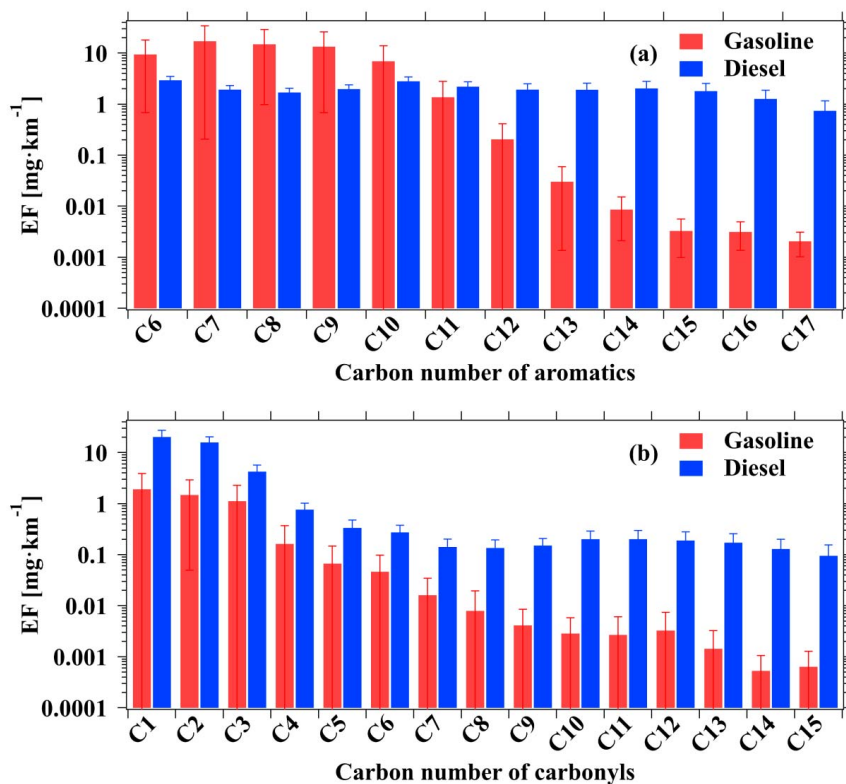
830 **Figure 7.** Scatterplot of VOCs emission factors between gasoline and diesel vehicles.

831 Each data point indicates a VOC species measured by PTR-ToF-MS. The blue line is

832 the fitted result for all data points. The black line represents 1:1 ratio, and the shaded

833 areas represent ratios of a factor of 10 and 100.

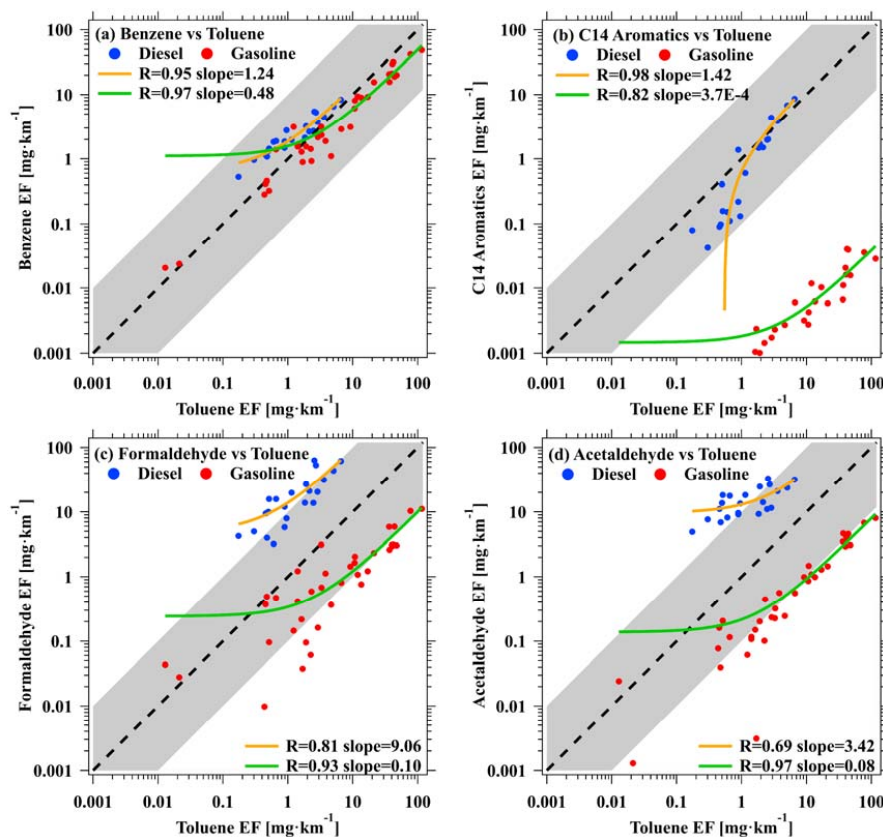
834



835

836 **Figure 8.** The determined emission factors of (a) aromatics and (b) carbonyls for each
837 carbon number from gasoline and diesel vehicles. Error bars represent standard
838 deviations of the emission factors for the VOCs of different carbon number.

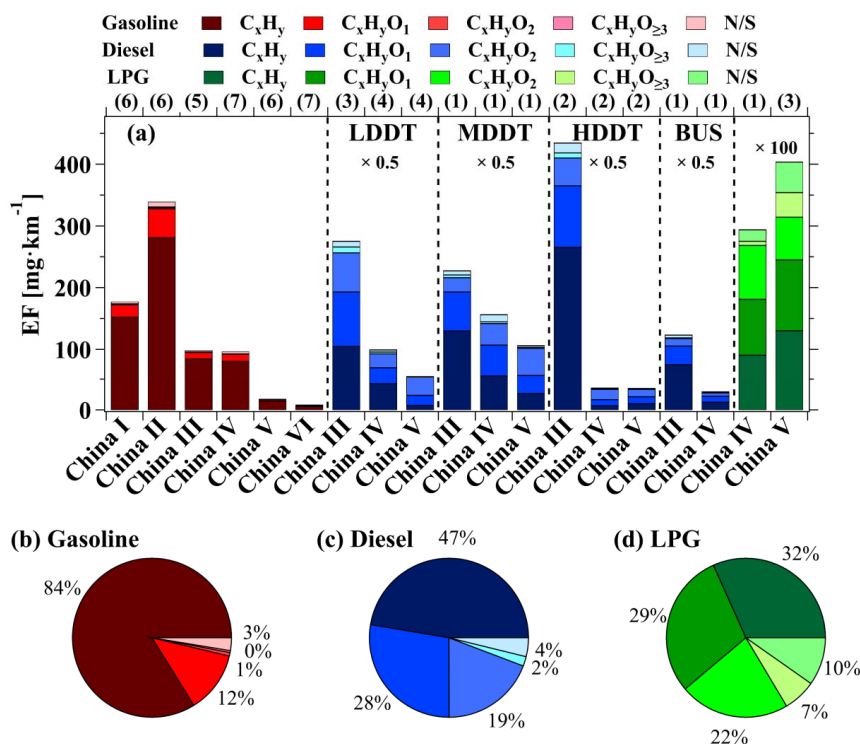
839



840

841 **Figure 9.** Scatterplots of the determined mileage-based emission factors of (a) benzene
842 versus toluene, (b) C₁₄ aromatics versus toluene, (c) formaldehyde versus toluene, and
843 (d) acetaldehyde versus toluene for gasoline and diesel vehicles. Each data point
844 represents each test vehicle in this study. The green and orange lines are the fitted results
845 for gasoline and diesel vehicle. The black line represents 1:1 ratio, and the shaded areas
846 represent ratio of a factor of 10.

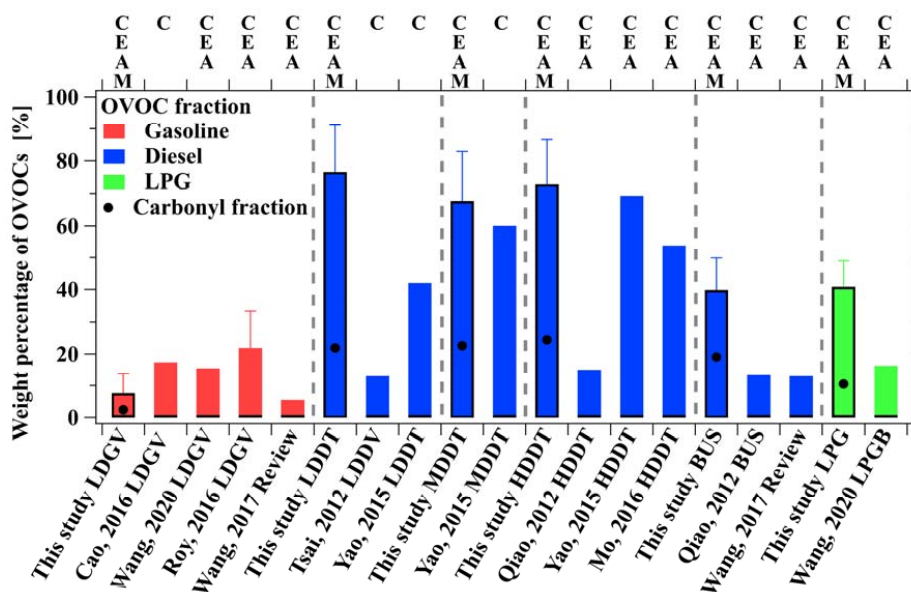
847



848

849 **Figure 10.** (a) The determined average emission factors for different emission standard
 850 from gasoline, diesel (×0.5), and LPG (×100) vehicles measured by PTR-ToF-MS. The
 851 different ion categories are discussed in the manuscript. Fractions of the determined
 852 average emission factors of VOCs ions in different ion categories from (b) gasoline, (c)
 853 diesel, and (d) LPG vehicles. The numbers above the top axis represent the number of
 854 all experiments (including multiple measurements for individual test vehicle) for each
 855 emission standard.

856



857

858 **Figure 11.** Comparison of OVOCs fractions determined in this study and those in
 859 previous studies. Error bars represent the standard deviations of the weight percentage
 860 of OVOCs. The C, E, A, M above the top axis represent the four groups of OVOCs
 861 measured in this study or previous studies, including Carbonyl: C, Ester/Ether: E,
 862 Alcohol: A, Multiple-functional: M.